

Applications of deep learning to relativistic hydrodynamics

Hengfeng Huang,^{1,2} Bowen Xiao,³ Ziming Liu,¹ Zeming Wu,^{1,2} Yadong Mu,^{3,4} and Huichao Song^{1,2,5}

¹*Department of Physics and State Key Laboratory of Nuclear Physics and Technology, Peking University, Beijing 100871, China*

²*Collaborative Innovation Center of Quantum Matter, Beijing 100871, China*

³*Institute of Computer Science and Technology, Peking University, Beijing 100080, China*

⁴*Center for Data Science, Peking University, Beijing 100871, China*

⁵*Center for High Energy Physics, Peking University, Beijing 100871, China*

(Dated: March 19, 2022)

Relativistic hydrodynamics is a powerful tool to simulate the evolution of the quark gluon plasma (QGP) in relativistic heavy ion collisions. Using 10000 initial and final profiles generated from 2+1-d relativistic hydrodynamics VISH2+1 with MC-Glauber initial conditions, we train a deep neural network based on **stacked U-net**, and use it to predict the final profiles associated with various initial conditions, including MC-Glauber, MC-KLN, AMPT and TRENTo. A comparison with the VISH2+1 results shows that the network predictions can nicely capture the magnitude and inhomogeneous structures of the final profiles, and nicely describe the related eccentricity distributions $P(\epsilon_n)$ ($n=2, 3, 4$). These results indicate that deep learning technique can capture the main features of the non-linear evolution of hydrodynamics, showing its potential to largely accelerate the event-by-event simulations of relativistic hydrodynamics.

I. INTRODUCTION

In recent years deep learning [1–3] has achieved great success in both daily life and in sciences. In particular, deep learning methods have been implemented to various research areas in physics, including the search of gravitational lens[4, 5], identifying and classifying the phases of Ising model [6–9], solving the quantum many body problem [10, 11], etc. In high energy physics, it has been applied to the search of Higgs and exotic particles [12, 13], classification of jet structure [14–16], etc. In the field of relativistic heavy-ion collisions, machine learning and deep neural networks have been employed to attack the problems of identifying the equation of state of hot QCD matter [17], jet-flavor classification in heavy-ion collisions [18], distinguishment between spinodal and Maxwell first-order phase transition [19], detecting nuclear shape deformation [20], Bayesian extraction of transport properties of the hot QCD matter [21–24], the phase diagram of two-dimensional complex scalar field theory [25], and principal component analysis of collective flow [26–32].

In this paper, we will apply deep learning to relativistic hydrodynamics, which is a useful tool to simulate the macroscopic evolution of relativistic systems in high energy nuclear physics and astrophysics [33]. Relativistic hydrodynamics solves the transport equations of the energy momentum tensor and charge currents based on the conservation laws. In relativistic heavy ion collisions, it has nicely described and predicted various flow data of the quark-gluon plasma (QGP), which played an important role in the discovery of the strongly coupled QGP and its nearly perfect fluid nature [21–24, 34–46]. However, traditional hydrodynamic simulations are time consuming. For example, the calculation of various flow harmonics requires ~ 1000 event-by-event hydrodynamic simulations, which takes ~ 500 and ~ 10000 cpu hours for the typical 2+1-d and 3+1-d simulations, respec-

tively [38–40, 47]. Basically, relativistic hydrodynamics translate the initial conditions to final profiles through solving a set of non-linear differential equations. In this work, we will explore whether the deep neural network could capture the main features of the non-linear evolution of 2+1-d hydrodynamics, and the possibilities to accelerate the related event-by-event simulations. Close to this work are Bayesian emulators [24, 48], which are powerful in constraining equation of states and transport coefficients, yet are not designed to predict the whole profiles of energy density and flow velocity.

It is worthwhile to mention that the interdisciplinary contributions of this work are two-fold: from the physics perspective, we speed up hydrodynamic simulations times with a deep neural network, while still capturing the details for the final profiles of the expanding QGP; On the other hand from the machine learning angle, we highlight the expressive power of the **stacked U-net** model, as well as its ability to approximate partial differential equation (PDE) in this particular task of relativistic hydrodynamics.

The paper is organized as follows: In Section II, we introduce the relativistic hydrodynamics and network design. In Section III, we show the results obtained from the network, followed by the discussions and conclusions in Section IV.

II. MODELS

A. Relativistic hydrodynamics

In this paper, we focus on relativistic ideal hydrodynamics with zero viscosity and charge densities, which solves the transport equations of the energy momentum tensor $T^{\mu\nu}$:

$$\partial_\mu T^{\mu\nu} = 0 \quad (1)$$

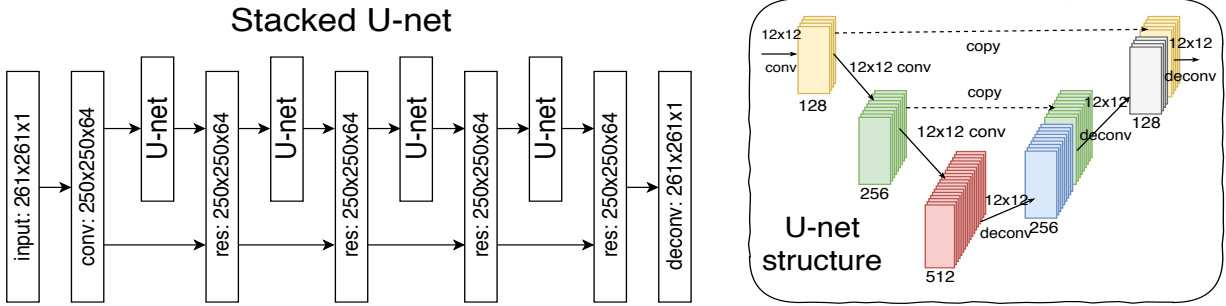


FIG. 1. An illustration of the encode-decode network, **stacked U-net**, which consists of the input and out layers and four residual U-net blocks. The right figure shows the U-net structure, and the depth of the hidden layer is written on the top of them.

where $T^{\mu\nu} = (e+p)u^\mu u^\nu - pg^{\mu\nu}$, e is the energy density, p is the pressure, and u^μ is the four velocity with $u^\mu u_\mu = 1$. With an assumption of longitudinal boost invariance, we solve the 2+1-dimensional hydrodynamic equations with an ideal EoS $p = \frac{e}{3}$, using the code **VISH2+1** [47, 49] [50]. The initial energy density profiles can be generated by some initial condition models, such as **MC-Glauber** [51, 52], **MC-KLN** [52–54], **AMPT** [55–57] and **TRENT0** [58] with zero initial transverse flow velocity. We run **VISH2+1** with three selected fixed evolution times $\tau - \tau_0 = 2.0, 4.0$ and 6.0 fm/c ($\tau_0 = 0.6$ fm/c) to obtain the energy momentum tensor $T^{\tau\tau}(\tau, x, y)$, $T^{\tau x}(\tau, x, y)$, $T^{\tau y}(\tau, x, y)$ profiles at these times. For numerical accuracy, the time step and grid sizes of the simulations are set to $d\tau = 0.04$ fm/c and $dx = dy = 0.1$ fm, within a fixed transverse area of $13 \text{ fm} \times 13 \text{ fm}$ that have been used to describe the typical QGP expansion in relativistic heavy ion collisions.

B. Network design

For deep learning, the initial and final energy momentum tensor $T^{\tau\tau}$, $T^{\tau x}$, $T^{\tau y}$ profiles from hydrodynamics are treated as initial and final image sets with 261×261 pixels. In practice, we first run the event-by-event hydrodynamic simulations to obtain 10000 initial and final image sets, then use them to train the deep neural network, which aims at achieving nice predictions of the final energy density and flow velocity profiles for other input initial conditions.

The related network we adopted in this work is the **stacked U-net (sU-net)** [59], which is a variation of the traditional encoder-decoder network that could enhance gradient flow in the deeper part of the network during back propagation. Fig. 1 presents an intuitional view of the network structure. It consists of 4 serially connected U-net blocks with residual connections between them. Each U-net block has 3 convolution layers and 3 deconvolution layers. In each U-net block, the output of the first two convolution layers are also fed into the last two deconvolution layers respectively by concatenating the feature maps along the channel dimension. The ac-

tivation function for all layers except for the output one is *Leaky ReLU* $f(x) = \max\{x, 0.03x\}$, while that for the output layer is *softplus* $f(x) = \ln(1 + e^x)$ for $T^{\tau\tau}$ mapping and $f(x) = x$ for $T^{\tau x}$ and $T^{\tau y}$ mapping. To make the network focus more on local patterns, we set the kernel size of all convolution and deconvolution layers to 3×3 . The loss function of the network is *normalized MAE loss* $Loss = \frac{|y_1 - y_0|}{|y_0|}$, where y_1 is the output of the network and y_0 is the ground truth. We use the standard mini-batch stochastic gradient descent algorithm for optimization. The batch size for training is 16 and learning rate exponentially decays from 10^{-3} to 10^{-5} . Each weight is randomly initialized from the uniform distribution on $[-0.001, 0.001]$ and each bias is set to zero. Our code is built with TensorFlow and the training process runs for about 1 day on a machine with single NVIDIA Tesla P40 GPU, using 10000 “initial” and “final” profiles from **VISH2+1** hydrodynamic simulations.

We have noticed that, although one trained **sU-net** can make nice predictions for shorter hydrodynamic evolution, it fails to accurately predict the final profiles of longer evolution time ($\tau - \tau_0 > 4.0$ fm/c) from the initial profiles at τ_0 . Considering that the evolving QGP system is highly non-linear and tends to smear-out its initial structures during longer evolution, we divide the whole evolution time $\tau - \tau_0$ into n parts with equal time interval $\Delta\tau$: $\tau - \tau_{n-1} \dots \tau_2 - \tau_1, \tau_1 - \tau_0$. For each evolution part, we train an individual **sU-net** using the corresponding “initial” and “final” profiles from hydrodynamics. To predict the final profiles at τ from initial profiles at τ_0 , we first use the trained **sU-net-1** to predict the profiles at time τ_1 and then use them as the initial conditions for **sU-net-2** to predict the profiles at time τ_2 and so on. In this way, the combined **sU-net** series ($i=1\dots n$) mimic the hydrodynamic evolution with much larger time step $\Delta\tau$ that can not be managed by traditional hydrodynamic algorithm (In more detail, for the following evolution with $\tau - \tau_0 = 6.0$ fm/c, we set $n=3$ with $\Delta\tau = 2.0$ fm/c). Note that **sU-net-1**, **sU-net-2** and **sU-net-3** are not identical since the initial and final profiles are generated by **VISH2+1**, which implement the 2+1-d hydrodynamic equations explicitly depended

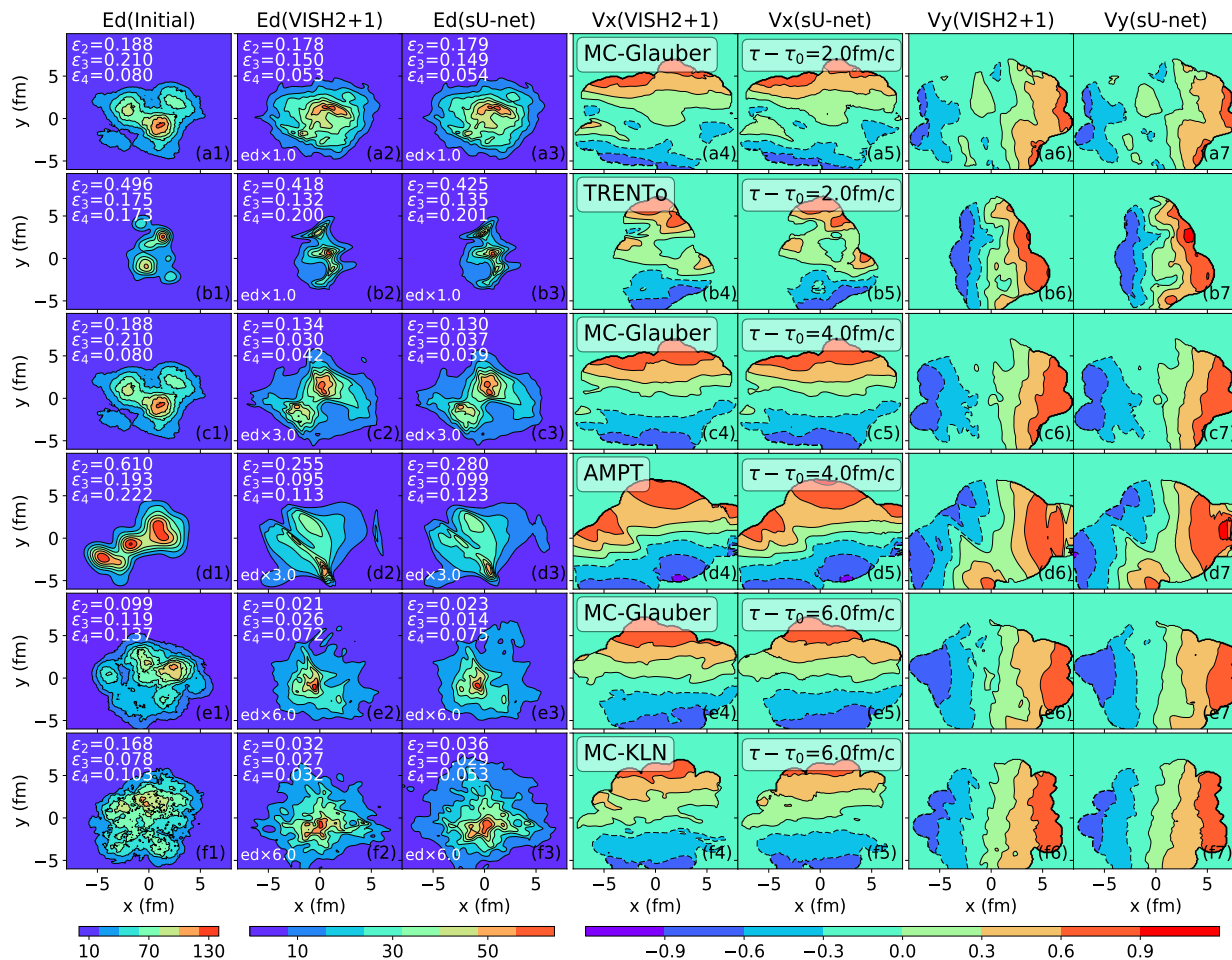


FIG. 2. Energy density and flow velocity profiles at $\tau - \tau_0 = 2.0, 4.0, 6.0$ fm/c, calculated from VISH2+1 and predicted by the network for six test cases with initial profiles generated from MC-Glauber, MC-KLN, AMPT and TRENTo.

on τ [49, 60].

III. RESULTS

As explained in the above text, we first use 10000 initial and final image sets from VISH2+1 with MC-Glauber initial conditions to train the combined **stacked U-net**, and then use the trained network to predict the final profiles from the initial profiles generated from MC-Glauber, MC-KLN, AMPT and TRENTo as tests. Fig. 2 presents a comparison between the results from VISH2+1 hydrodynamic evolution and the predictions from the network at $\tau - \tau_0 = 2.0, 4.0, 6.0$ fm/c for 6 selected test cases. It shows that the well designed and trained network could nicely predict the final states, which captures the structures of the contour plots for both final energy density and flow velocity. It is impressive that, although the network is trained with the initial and final image sets associated with the MC-Glauber initial conditions, it could still nicely predict the final profiles of other initial conditions with different fluctuation patterns, as shown in

panel (b), (d) and (f).

To further evaluate the predictive power of the network, we further calculate the eccentricity coefficients

$$\varepsilon_n = \frac{\int r dr d\phi r^n e(r, \phi) e^{in\phi}}{\int r dr d\phi r^n e(r, \phi)} \quad (n = 2, 3, 4) \quad (2)$$

for initial and final energy density $e(r, \phi)$ profiles, which are quantities commonly used to evaluate the deformation and inhomogeneity of the QGP fireball in relativistic heavy ion collisions [38–40, 47]. These values of ε_n ($n=2, 3, 4$) for these 6 selected test cases are written in the related panels (a-f). From Fig. 2 and the calculated values of ε_n ($n=2, 3, 4$), we have also noticed that differences between the hydrodynamic results and the network predictions increase for longer evolution time since the combined **sU-net** series tend to accumulate errors with more sU-net added.

Fig. 3 presents the eccentricity distributions $P(\varepsilon_n)$ for the energy density profiles at evolution times $\tau - \tau_0 = 2.0$ fm/c, 4.0 fm/c and 6.0 fm/c, calculated from VISH2+1 and predicted from the network for 10000 tested initial profiles generated from MC-Glauber, MC-KLN, AMPT and

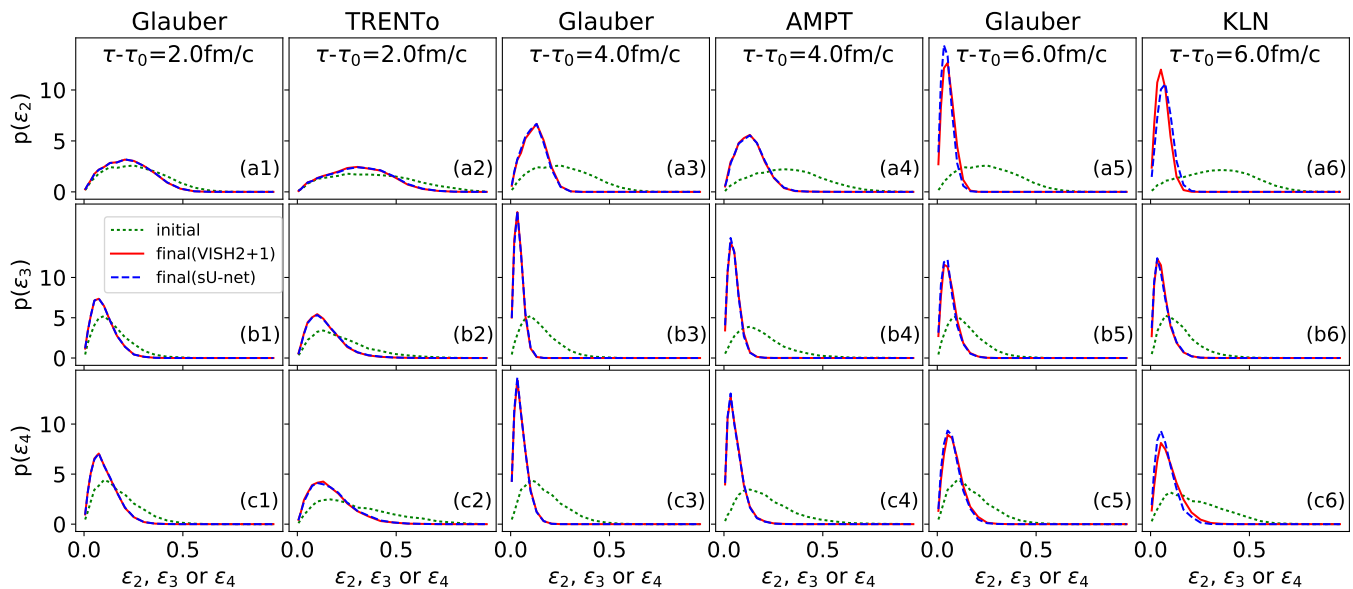


FIG. 3. Eccentricity distribution $P(\varepsilon_n)$ ($n=2, 3, 4$), at $\tau - \tau_0 = 2.0, 4.0, 6.0$ fm/c, calculated from VISH2+1 and predicted by the network for 100000 tested initial profiles generated from MC-Glauber, MC-KLN, AMPT and TRENTo.

TRENTo. For all these tested cases, the final eccentricity distributions $P(\varepsilon_n)$ ($n=2, 3, 4$) from the network almost overlap with the ones from VISH2+1, which also obviously deviate from the initial eccentricity distributions $P_0(\varepsilon_n)$. In Fig. 4, scatter plots show event-by-event comparisons between true eccentricities of ‘final’ profiles and predicted ones, and histograms of errors are plotted in the inset figure.

We also find that, with the well trained network, the final state profiles can be speedily generated from the initial profiles. Compared with the 10-20 minute calculation time with traditional CPU for a single-event hydrodynamic evolution, the network takes several seconds to directly generate the final profile for different types of initial profiles with the P40 GPU, which shows the potential to accelerate the realistic event-by-event hydrodynamic simulations in the near future. However, given the fact that 50-100x speedup of hydro simulations can be already achieved by switching from CPU to GPU [61, 62], we believe there is still much room to improve our proof-of-concept first step in further studies.

IV. DISCUSSION AND CONCLUSION

Using 10000 initial and final energy momentum tensor profiles from VISH2+1 hydrodynamics with MC-Glauber initial conditions, we successfully trained a deep neural network based on **stacked U-net**, and use it to predict the final profiles for different initial conditions, including MC-Glauber, MC-KLN, AMPT and TRENTo. A comparison with the VISH2+1 results showed that the network predictions could nicely capture the magnitude and inhomogeneous structures of the final profiles, which also nicely de-

scribe the related eccentricity distributions $P(\varepsilon_n)$ ($n=2, 3, 4$). These results indicate that deep learning could capture the main feature of the non-linear evolution of hydrodynamics, which also shows the potential of largely accelerating the realistic event-by-event hydrodynamic simulations in relativistic heavy ion collisions.

In order to outline the highlights, as well as point out limitations of this work, we further explain the following characteristics that mark good works and provide guidelines for future studies.

Universality: Deep learning might not learn the realistic physics underlying the dataset. By contrast, sometimes its predictions are based on non-physical features in the dataset, as has been pointed out in [63]. In this work, we exclude such undesirable possibility by training our deep model on MC-Glauber initial conditions and test on results for other initial models including MC-KLN, AMPT and TRENTo.

Causality: Due to speed of light as an upper bound for all physical speeds, our neural network should satisfy such causal relations, otherwise it will produce non-physical results. The joint use of convolutional layers and the stacked structure elegantly handles this issue by allowing one pixel to influence its neighborhoods only. Such causality in convolutional layers is known as receptive field [64] in the machine learning literature. More concretely suppose our CNN has L layers with the i -th layer using convolutional filters of size $(2n_i+1) \times (2n_i+1)$, then it is reasonable to match the size of the receptive field $R_r = (\sum_i n_i) \Delta x$ (Δx is the grid length) with the size of light cone $R_l = c(\tau - \tau_0)$. If $R_r < R_l$, the expressivity of the neural network is bottlenecked; If $R_r > R_l$, the neural network is unnecessarily expressive which might lead to longer training time.

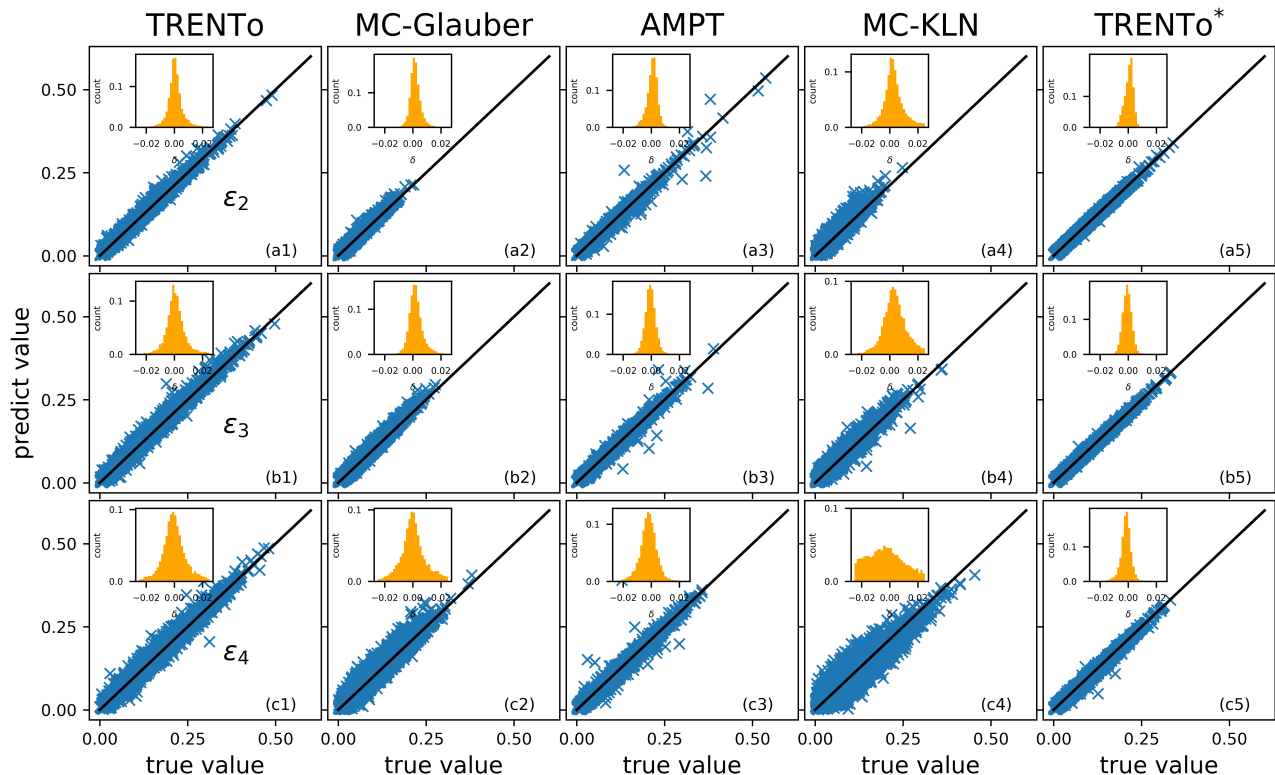


FIG. 4. Event-by-event comparisons of eccentricities ε_n ($n=2, 3, 4$) at $\tau - \tau_0 = 6.0$ fm/c, calculated from VISH2+1 and predicted by the network for 100000 tested initial profiles generated from MC-Glauber, AMPT, MC-KLN, and TRENTo (with two set of parameters distinguished by *).

Utility: One limitation of this work is the fixed time output. Future works will consider more flexible architectures (e.g. physics-informed neural network in [65]) to obtain the energy-momentum tensor at the freeze-out surface with more realistic implementation in heavy ion collisions.

Interpretability: Another minor limitation of the stacked U-net model lies in the lack of interpretability. In future works, we will investigate the possibilities of encoding physics explicitly in network design, as in [65]. Efforts on gaining interpretability of deep learning in heavy-ion collisions include [17, 20].

In summary, our current investigations mainly focus on mimicking the 2+1-dimensional hydrodynamic evolution with fixed evolution time, using the deep learning technique. On the one hand, for more realistic implementation to relativistic heavy ion collisions, it is worthwhile to explore the possibilities of mapping

the initial profiles to the final profiles on the freeze-out surface with fixed energy density as well as extending the related investigations to 3+1-dimensional simulations. On the other hand, it is also worthwhile to develop computational tools that are more transparent for scientific evaluations, where a possible way is to encode physical prior (the functional form of the PDE, boundary conditions etc.) into the network architecture.

V. ACKNOWLEDGMENTS

We thank the discussions from L. G. Pang, K. Zhou and X.-N. Wang. H. H., Z. L. and H. S. are supported by the NSFC under grant No. 11675004 and No. 12075007. B. X. and Y. M. are supported by NSFC under grant no. 61772037.

[1] I. Goodfellow, Y. Bengio, and A. Courville, *Deep Learning* (MIT Press, 2016) <http://www.deeplearningbook.org>.

[2] Y. LeCun, Y. Bengio, and G. Hinton, *nature* **521**, 436 (2015).

[3] D. Silver, A. Huang, C. J. Maddison, A. Guez, L. Sifre, G. Van Den Driessche, J. Schrittwieser, I. Antonoglou,

- V. Panneershelvam, M. Lanctot, *et al.*, *nature* **529**, 484 (2016).
- [4] Y. D. Hezaveh, L. P. Levasseur, and P. J. Marshall, *Nature* **548**, 555 (2017).
- [5] C. E. Petrillo *et al.*, *Mon. Not. Roy. Astron. Soc.* **472**, 1129 (2017).
- [6] N. Sun, J. Yi, P. Zhang, H. Shen, and H. Zhai, *Physical Review B* **98**, 085402 (2018).
- [7] J. Carrasquilla and R. G. Melko, *Nature Physics* **13**, 431 (2017).
- [8] E. P. Van Nieuwenburg, Y.-H. Liu, and S. D. Huber, *Nature Physics* **13**, 435 (2017).
- [9] P. Broecker, J. Carrasquilla, R. G. Melko, and S. Trebst, *Scientific reports* **7**, 8823 (2017).
- [10] G. Carleo and M. Troyer, *Science* **355**, 602 (2017).
- [11] X. Gao and L.-M. Duan, *Nature communications* **8**, 662 (2017).
- [12] P. Baldi, P. Sadowski, and D. Whiteson, *Nature communications* **5**, 4308 (2014).
- [13] P. Baldi, K. Cranmer, T. Faucett, P. Sadowski, and D. Whiteson, *The European Physical Journal C* **76**, 235 (2016).
- [14] J. Cogan, M. Kagan, E. Strauss, and A. Schwartzman, *JHEP* **02**, 118 (2015).
- [15] P. Baldi, K. Bauer, C. Eng, P. Sadowski, and D. Whiteson, *Physical Review D* **93**, 094034 (2016).
- [16] A. Chakraborty, S. H. Lim, and M. M. Nojiri, *Journal of High Energy Physics* **2019**, 135 (2019).
- [17] L.-G. Pang, K. Zhou, N. Su, H. Petersen, H. Stöcker, and X.-N. Wang, *Nature communications* **9**, 210 (2018).
- [18] Y.-T. Chien, *Nuclear Physics A* **982**, 619 (2019).
- [19] J. Steinheimer, L.-G. Pang, K. Zhou, V. Koch, J. Randrup, and H. Stoecker, *Journal of High Energy Physics* **2019**, 122 (2019).
- [20] L.-G. Pang, K. Zhou, and X.-N. Wang, *arXiv preprint arXiv:1906.06429* (2019).
- [21] J. E. Bernhard, J. S. Moreland, S. A. Bass, J. Liu, and U. Heinz, *Phys. Rev. C* **94**, 024907 (2016).
- [22] J. E. Bernhard, J. S. Moreland, and S. A. Bass, *Nature Phys.* **15**, 1113 (2019).
- [23] D. Everett *et al.* (JETSCAPE), (2020), *arXiv:2010.03928 [hep-ph]*.
- [24] D. Everett *et al.* (JETSCAPE), (2020), *arXiv:2011.01430 [hep-ph]*.
- [25] K. Zhou, G. Endrődi, L.-G. Pang, and H. Stöcker, *Physical Review D* **100**, 011501 (2019).
- [26] R. S. Bhalerao, J.-Y. Ollitrault, S. Pal, and D. Teaney, *Phys. Rev. Lett.* **114**, 152301 (2015).
- [27] A. Mazeliauskas and D. Teaney, *Physical Review C* **91**, 044902 (2015).
- [28] A. M. Sirunyan, A. Tumasyan, W. Adam, F. Ambrogio, E. Asilar, T. Bergauer, J. Brandstetter, E. Brondolin, M. Dragicevic, J. Erö, *et al.*, *Physical Review C* **96**, 064902 (2017).
- [29] Z. Liu, W. Zhao, and H. Song, *The European Physical Journal C* **79**, 870 (2019).
- [30] Z. Liu, A. Behera, H. Song, and J. Jia, *Phys. Rev. C* **102**, 024911 (2020).
- [31] F. G. Gardim, F. Grassi, P. Ishida, M. Luzum, and J.-Y. Ollitrault, *Phys. Rev. C* **100**, 054905 (2019).
- [32] I. Altsybeev, *Journal of Physics: Conference Series* **1602**, 012004 (2020).
- [33] L. D. Landau and E. M. Lifshitz, (Elsevier, 2013).
- [34] M. Gyulassy and L. McLerran, *Nuclear Physics A* **750**, 30 (2005).
- [35] B. Müller and J. L. Nagle, *Annu. Rev. Nucl. Part. Sci.* **56**, 93 (2006).
- [36] P. Huovinen, in *Quark-Gluon Plasma 3* (World Scientific, 2004) pp. 600–633.
- [37] P. F. Kolb and U. Heinz, in *Quark-Gluon Plasma 3* (World Scientific, 2004) pp. 634–714.
- [38] U. Heinz and R. Snellings, *Annual Review of Nuclear and Particle Science* **63**, 123 (2013).
- [39] C. Gale, S. Jeon, and B. Schenke, *International Journal of Modern Physics A* **28**, 1340011 (2013).
- [40] H. Song, Y. Zhou, and K. Gajdošová, *Nuclear Science and Techniques* **28**, 99 (2017).
- [41] B. Müller, J. Schukraft, and B. Wyslouch, *arXiv preprint arXiv:1202.3233* **1**.
- [42] H. Song, S. A. Bass, U. Heinz, T. Hirano, and C. Shen, *Phys. Rev. Lett.* **106**, 192301 (2011).
- [43] B. Schenke, S. Jeon, and C. Gale, *Phys. Rev. Lett.* **106**, 042301 (2011).
- [44] C. Gale, S. Jeon, B. Schenke, P. Tribedy, and R. Venugopalan, *Phys. Rev. Lett.* **110**, 012302 (2013).
- [45] X. Zhu, Y. Zhou, H. Xu, and H. Song, *Phys. Rev. C* **95**, 044902 (2017).
- [46] W. Zhao, H.-j. Xu, and H. Song, *Eur. Phys. J. C* **77**, 645 (2017).
- [47] C. Shen, Z. Qiu, H. Song, J. Bernhard, S. Bass, and U. Heinz, *Computer Physics Communications* **199**, 61 (2016).
- [48] S. Pratt, E. Sangaline, P. Sorensen, and H. Wang, *Phys. Rev. Lett.* **114**, 202301 (2015).
- [49] H. Song and U. Heinz, *Physical Review C* **77**, 064901 (2008).
- [50] In (τ, x, y, η) coordinate ($\tau = \sqrt{t^2 - z^2}$ and $\eta = \frac{1}{2} \ln \frac{t+z}{t-z}$), the energy density and pressure from 2+1-d hydrodynamics are longitudinal boost-invariant without a dependence on η , $e=e(\tau, x, y)$ and $p=p(\tau, x, y)$. Correspondingly, the four flow velocity are expressed as $\gamma_{\perp}(1, v^x(\tau, x, y), v^y(\tau, x, y), 0)$ with $v^{\eta} = 0$ [36, 37].
- [51] M. L. Miller, K. Reygers, S. J. Sanders, and P. Steinberg, *Annu. Rev. Nucl. Part. Sci.* **57**, 205 (2007).
- [52] T. Hirano and Y. Nara, *Physical Review C* **79**, 064904 (2009).
- [53] H.-J. Drescher and Y. Nara, *Physical Review C* **75**, 034905 (2007).
- [54] H.-J. Drescher and Y. Nara, *Physical Review C* **76**, 041903 (2007).
- [55] L. Pang, Q. Wang, and X.-N. Wang, *Physical Review C* **86**, 024911 (2012).
- [56] H.-j. Xu, Z. Li, and H. Song, *Physical Review C* **93**, 064905 (2016).
- [57] W. Zhao, Y. Zhou, H. Xu, W. Deng, and H. Song, *Phys. Lett. B* **780**, 495 (2018).
- [58] J. S. Moreland, J. E. Bernhard, and S. A. Bass, *Physical Review C* **92**, 011901 (2015).
- [59] K. He, X. Zhang, S. Ren, and J. Sun, in *Proceedings of the IEEE conference on computer vision and pattern recognition* (2016) pp. 770–778.
- [60] H. Song, *Causal Viscous Hydrodynamics for Relativistic Heavy Ion Collisions*, Other thesis (2009), *arXiv:0908.3656 [nucl-th]*.
- [61] L.-G. Pang, H. Petersen, and X.-N. Wang, *Phys. Rev. C* **97**, 064918 (2018).

- [62] D. Bazow, U. W. Heinz, and M. Strickland, *Comput. Phys. Commun.* **225**, 92 (2018).
- [63] P. Zhang, H. Shen, and H. Zhai, *Physical review letters* **120**, 066401 (2018).
- [64] W. Luo, Y. Li, R. Urtasun, and R. Zemel, in *Advances in neural information processing systems* (2016) pp. 4898–4906.
- [65] M. Raissi, P. Perdikaris, and G. E. Karniadakis, *Journal of Computational Physics* **378**, 686 (2019).